Tunable 2D hexagonal phase array in domain engineered z-cut lithium niobate crystal

M. Paturzo*, P. De Natale, S. De Nicola, P. Ferraro
Istituto Nazionale di Ottica Applicata del CNR and LENS-European Laboratory for Nonlinear Spectroscopy, Via Campi Flegrei 34, 80078 Pozzuoli (Na), Italy

S. Mailis, R.W. Eason
Optoelectronics Research Centre, University of Southampton, Highfield, Southampton, SO17 1BJ, UK

G. Coppola, M. Iodice, M. Gioffré
Istituto Microelettronica e Microsistemi del CNR, Via P. Castellino 111, 80131, Napoli, Italy

Abstract

An optical phase array with tunable phase step is demonstrated. The phase array consists of a 2-dimensional hexagonal lattice of inverted ferroelectric domains fabricated on a z-cut lithium niobate substrate. The electro-optically tunable phase step is obtained by the application of an external electric field along the z axis of the crystal via transparent electrodes. Theoretical analysis and experimental results are presented showing that a tunable and flexible adaptive optical illuminator device can be realized by combining the electro-optic tunability with the Talbot effect. Generation of a multiplicity of light pattern is shown.

OCIS codes: 050.1950, 070.6760, 230.2090.

*E-mail: melania.paturzo@inoa.it

Array illuminators are devices that transform a plane wave into a periodic optical intensity pattern, therefore have great potentiality that can be exploited in different fields of applications such as spatially addressed multiplexing in optical telecommunications or optical testing using Hartman methods [1,2].

Different optical elements can be used to obtain the array of light spot such as diffractive gratings, i.e. Dammann gratings or lenslet–arrays [3,4]. Among the various different configurations, the mostly used devices are the so named Talbot illuminators (TI), based on the Talbot effect [5]. In the past years TIs have been extensively studied and nowadays are considered ones of the more simple and efficient devices in the field of optical information processing [6,7,8]. Recently, hexagonal phase arrays (HPA) has been the subject of investigation since the hexagonal geometry is widely used in optical devices such as fibre-bundles, detector arrays, photonic delay lines in optical communication, etc...[9]. The conventional method for fabrication of phase step array illuminators is the spatially selective etching to vary the optical path length, hence the phase, as in the case of one dimensional phase masks. However, in this way the phase step is optimized for a specific wavelength and is fixed since it is defined by the etch depth of the periodic structure of the array.

In this letter we present an adaptive and dynamic hexagonal electro-optic phase step array fabricated from a lithium niobate substrate which allows high damage threshold transmission over a wide spectral range, from the infra red to the near UV (5μm-400nm). The fabricated device consists of a 2-dimensional (2D) array of periodically inverted ferroelectric domains, along the z-axis, in a lithium niobate sample. The phase step between opposite ferroelectric domains is achieved via the application of an external electric field, along the z-axis, through transparent electrodes covering the opposite z-faces of the crystal. The electro-optically induced refractive index change depends on the ferroelectric domain orientation; hence differential phase shift can be achieved for parts of a beam propagated through opposite

domains. One important property of this new proposed configuration of TI is the intrinsic flexibility in terms of tunability. Due to the electro-optic effect, the phase step can be changed continuously over all the 0-2π range by applying a variable voltage (e.g. a linear ramp). Moreover, it can be optimized for any optical wavelength within the working spectral range of the crystal. Another very important feature of our device in comparison with the case of a fixed phase step is also the fine control obtainable over the step. In fact, in a conventional phase array illuminator, when the specific depth is provided by the fabrication process according to its design, it is clear that any change of temperature, through the thermo-optic effect could change the refractive index of the device and consequently the phase step. In our case the phase step can be actively controlled and corrected in real time to compensate for changes of the ambient conditions.

Finally, it is important to underline that the proposed configuration shows some advantages also compared with spatial light modulators (SLM) based for example on liquid crystals. In fact, the pixel size of our device (the size of individual inverted domains) can be as small as a couple of microns, which is the current limit for bulk ferroelectric domain inversion with conventional methods, this value is at least two orders of magnitude smaller than the actually available SLM [10,11].

We realized a first demonstrator which consists of a 2D array of inverted ferroelectric domains arranged in a hexagonal lattice (HexLN). The configuration can be easily expanded to cover arbitrary 2D lattices. Moreover, further ability to control each pixel individually will expand even more the flexibility for the reproduction of arbitrary phase patterns.

Hexagonally poled samples are prepared by standard electric field poling at room temperature [12]. For the ferroelectric domain inversion, the z- face of a 0.5 μm thick z-cut lithium niobate crystal sample is covered with photoresist and then photo-lithographically patterned with a 2D array of hexagonal openings arranged in a hexagonal lattice. Fig. 1a shows a section of the

photolithography mask used in the fabrication process. External electric field, higher than the coercive field, is applied via conductive gel electrodes between the two opposite z faces of the crystal while the current is monitored in order to control the domain inversion process. After the poling process, a 2D hexagonal lattice of domains, that is a replica of the photolithographic pattern, is created. An optical microscopy image of the actual domain structure visualized is shown in Fig. 1b. The structure, shown in Fig. 1b, is very similar to the photolithography mask pattern of Fig. 1a in terms of the domain period. However, there is some difference between the domain inverted pattern and the mask due to sideway domain spreading during the poling process. The distance between neighbouring hexagons is 35 μm and the overall domain inverted region covers an area of approximately 2 cm^2.

Transparent ITO electrodes are deposited on the opposite z faces of the poled crystal so that external field can be applied across the sample without disturbing the optical transmission along the z axis. The 514.5 nm line of an Ar+ ion laser is used to study the near field diffraction pattern from the sample. The laser beam was spatially filtered, expanded and re-collimated covering the entire 2 cm^2 periodically poled area as shown in Fig.2.

A microscope objective lens was used to magnify and project the near field diffraction pattern onto a CCD camera enabling the monitoring of the near field intensity pattern variations at different planes of the Talbot length and for different values of the applied voltage.

The performance of a variable phase step device based on a 2D HPA has been studied theoretically by modelling the propagation of a plane wave through the structure along the z axis of the crystal. The transmittance of an HPA placed in the $z = 0$ plane can be written in terms of convolution:

$$t(x,y) = u(x,y) \otimes \frac{1}{t_x t_y}\left[comb(x/t_x)comb(y/t_y) + comb(x/t_x - 1/2)comb(y/t_y - 1/2)\right] \qquad (1)$$

where the *comb* function is a sequence of infinite delta impulses uniformly distributed in space, t_x and $t_y = \sqrt{3}t_x$ are the periods of the HPA along the x and y directions, respectively, and $u(x,y)$ is the transmittance of one of its period. As a result of the poling process the phase grating consists of hexagonal domains with opposite polarization inside and outside the hexagons, respectively. Applying an external voltage to the crystal, the refractive index $n_0 = 2.33$ changes by $\Delta n = -(1/2d)r_{13}n_0^3 V$ where r_{13} is the appropriate element of the electro-optic tensor, d the thickness of the crystal and V is the applied voltage.

For a monochromatic plane wave of wavelenth λ, incident on the HPA, the voltage application causes a spatially dependent phase shift $\Delta\phi$ given by the relation $\lambda\Delta\phi/2\pi = \pm(d\cdot\Delta n + (n_0 - 1)d_{33}V)$ where $d_{33}V$ is the piezoelectric thickness change $(d_{33} = 7.57\times10^{-12}\ \mathrm{m/V})$ generated by the applied voltage and the $\pm$ accounts for the opposite sign in the areas of opposite ferroelectric polarization. Therefore, the total phase change across the hexagonal domain walls is $2\Delta\phi$. Accordingly, the transmitted field of the basic periodic element of the HPA can be written, omitting a common phase factor, as $u(x,y) = \exp[\pm i\Delta\phi]$ and from Eq.(1), the diffracted field $u_z(\Delta\phi;x,y)$ at the z plane can be expressed in the following Fourier series expansion:

$$u_z(\Delta\phi;x,y) = \sum_{n,m} c_{nm}(\Delta\phi)\exp\left[i2\pi\left(\frac{nx}{t_x}+\frac{my}{t_y}\right)\right]\exp\left[i\pi\lambda z\left(\frac{n^2}{t_x^2}+\frac{m^2}{t_y^2}\right)\right] \qquad (2)$$

Equation (2) shows that the intensity distribution $|u_z|^2$ at the z plane is determined by the applied external electric field, through the dependence of the complex coefficients $c_{nm}(\Delta\phi)$ on the induced phase shift. For the designed phase grating we have $t_x = 5l/2 = 35$ μm where $l = 14$ μm is the side of the hexagonal areas. The coefficients $c_{nm}(\Delta\phi)$ appearing in Eq. (2) can be explicitly calculated, namely:

$$c_{00}(\Delta\phi) = \exp[-i(\Delta\phi)] + \alpha\left(\exp[i(\Delta\phi)] - \exp[-i(\Delta\phi)]\right) \tag{3a}$$

$$c_{nm}(\Delta\phi) = i(1+\exp[i\pi(n+m)])\frac{(-1)^n \sin(\Delta\phi)}{n(n^2-m^2)\pi^2}\times \left((n+m)\cos\left(\frac{2m-3n}{5}\pi\right) - 2n\cos\left(\frac{n\pi}{5}\right) + (n-m)\cos\left(\frac{2m+3n}{5}\pi\right)\right) \tag{3b}$$

Where the parameter $\alpha = 12/25 \approx 0.48$ in the zero-*th* component c_{00}, is the compression ratio of our HPA, i.e., the ratio of the area of the phase $\Delta\phi$ to the whole area of the period. Eq. (3b) shows that the coefficients c_{nm} are equal to zero when $m+n$ is an odd integer and $|m|+|n| \neq 0$ and that their amplitude is modulated by the same phase dependent term, $\sin(\Delta\phi)$. The maximum contrast is obtained when $\Delta\phi = \pi/2$, i.e. when the overall phase change is π.

At the Talbot distance $z_t = 3t_x^2/2\lambda = 3.6\,\text{mm}$ we have that $u_z(\Delta\phi; x, y)$ is equal to incident field $t(x, y)$. On the basis of the above analysis we have made some experimental tests to demonstrate that the device can be used to produce different kind of patterns with different geometrical arrangements. Figs.3 and 4 shows typical patterns generated by the HPA.

The theoretically predicted and experimentally obtained patterns are shown in Fig. 3 for three values of distances, i.e. $z = z_t/2 = 1.8$ mm, corresponding to half Talbot distance, $z = z_t/4 = 0.9\,\text{mm}$ and $z = z_t/8 = 0.45\,\text{mm}$ and for two values of the total phase change, namely $2\Delta\phi = \pi$ and $2\Delta\phi = 3\pi/2$ corresponding to applied voltages $V_\pi = 2.4$ kV and $V_{3\pi/2} = 3.6$ kV, respectively. The agreement between the recorded intensity distribution and the theoretical patterns appears to be satisfactory. Different kinds of intensity distributions can be easily obtained depending on the recording conditions; for example, Fig.4 shows a variety

of interesting patterns that have been obtained at different voltage and recording distances from the array illuminator (a-3.7mm, 3.6 kV; b-0.5mm, -3.8 kV; c-1.0mm, -3.2 kV; d-0.5mm, 5.2 kV; e-1.5mm, 4.7 kV; f-3.0mm, 3.6 kV).

In conclusion in this paper has been shown the capability of a dynamic and electrooptically tunable 2D phase array used as a Talbot illuminator. It has been demonstrated that a variety of pattern can be generated under different voltage bias and distances and a theoretical model, that successfully reproduced the experimentally observed behaviour, has been developed. Such flexible array could be potentially used in a variety of applications such as optical interconnects, tunable lithographic masks or 2D optical trapping and assembling of particles. Further investigation will be devoted to investigate other geometries of PPLN structures and also to study the diffraction efficiency of the generated pattern for the specific applications.

Acknowledgements

This research was partially funded by the MIUR within the FIRB project n. RBNE01KZ94 "Microdispositivi fotonici in Niobato di Litio"and partially by the MIUR project n.77 DD N.1105/2002 " Circuiti fotonici integrati per le telecomunicazioni ottiche e la sensoristica".

References (complete)

1. N. Madamopoulos and N. A. Riza, "Demonstration of an All-Digital 7-Bit 33-Channel Photonic Delay Line for Phased-Array Radars ", Appl. Opt. **39**, 4168-4181 (2000).
2. D. Malacara, *Optical shop testing* (Wiley Interscience, New York, 1991).
3. H. Dammann and K. Gortler, "High-efficiency in-line multiple imaging by means of multiple phase holograms ", Opt. Comm. **3**, 312 (1971).
4. E. Bonet, P. Andres, J. C. Barreiro and A. Pons, "Self-imaging properties of a periodic microlens array – versatile array illuminator realization", Opt Comm. **106**, 39 (1994).
5. K. Patorski, *Handbook of the moirè fringe technique* (Elsevier, Amsterdam, 1993).
6. A. W. Lohmann and J. A. Thomas, "Making an array illuminator based on the Talbot effect", Appl. Opt. **29**, 4337-4340 (1990).
7. V. Arrizon and J. Ojeda-Castañeda, "Talbot array illuminator with binary phase gratings", Opt. Lett. **18**,1-3 (1993).
8. V. Arrizon and J. Ojeda-Castañeda, "Fresnel diffraction of substructctured gratings: matrix description" Opt. Lett. **20**, 118-120 (1995).
9. Peng Xi, Change Zhou, Enwen Dai and Liren Liu, "Generation of near-field hexagonal array illumination with a phase grating" Opt. Lett. **27**, 228-230 (2002).
10. K. L. Baker and E. A. Stappaerts, "A single-shot pixellated phase-shifting interferometer utilizing a liquid-crystal spatial light modulator," Opt. Lett. **31**, 733-735 (2006)
    http://www.opticsinfobase.org/abstract.cfm?URI=ol-31-6-733
11. M. S. Millán, J. Otón, and E. Pérez-Cabré, "Chromatic compensation of programmable Fresnel lenses," Opt. Express **14**, 6226-6242 (2006) http://www.opticsinfobase.org/abstract.cfm?URI=oe-14-13-6226

12. L.E.Myers, R.C.Eckardt, M.M. Fejer, R.L.Byer, W.R. Bosenberg, J.W. Pierce, "Quasi-phase-matched optical parametric oscillators in bulk periodically poled $LiNbO_3$", J. Opt. Soc. Am. B **12,** 2102-2115 (1995).

References (short)

1. N. Madamopoulos and N. A. Riza, Appl. Opt. **39**, 4168-4181 (2000).

2. D. Malacara, *Optical shop testing* (Wiley Interscience, New York, 1991).

3. H. Dammann and K. Gortler, Opt. Comm. **3**, 312 (1971).

4. E. Bonet, P. Andres, J. C. Barreiro and A. Pons, Opt Comm. **106**, 39 (1994).

5. K. Patorski, *Handbook of the moirè fringe technique* (Elsevier, Amsterdam, 1993).

6. A. W. Lohmann and J. A. Thomas, Appl. Opt. **29**, 4337-4340 (1990).

7. V. Arrizon and J. Ojeda-Castañeda, Opt. Lett. **18**,1-3 (1993).

8. V. Arrizon and J. Ojeda-Castañeda, Opt. Lett. **20**, 118-120 (1995).

9. Peng Xi, Change Zhou, Enwen Dai and Liren Liu, Opt. Lett. **27**, 228-230 (2002).

10. K. L. Baker and E. A. Stappaerts, Opt. Lett. **31**, 733-735 (2006).

11. M. S. Millán, J. Otón, and E. Pérez-Cabré, Opt. Express **14**, 6226-6242 (2006).

12. L.E.Myers, R.C.Eckardt, M.M. Fejer, R.L.Byer, W.R. Bosenberg, J.W. Pierce, J. Opt. Soc. Am. B **12,** 2102-2115 (1995).

Figures' captions

Fig. 1. Optical microscopy images of the photolithography mask used in the fabrication process (a), and of the actual domain structure (b).

Fig. 2. Scheme of the used optical set-up.

Fig.3. Experimental patterns obtained for a phase step $2\Delta\phi = \pi$ at $z = z_t / 2$ (a), $z = z_t / 4$ (b) and $z = z_t / 8$ (c) and the respective numerical simulations (d,e,f). Patterns obtained for a phase step $2\Delta\phi = 3\pi/2$ at $z = z_t / 2$ (g), $z = z_t / 4$ (h) and $z = z_t / 8$ (i) and the respective numerical simulations (l,m,n).

Fig. 4. A selection of interesting patterns obtained at different voltage and recording distances.

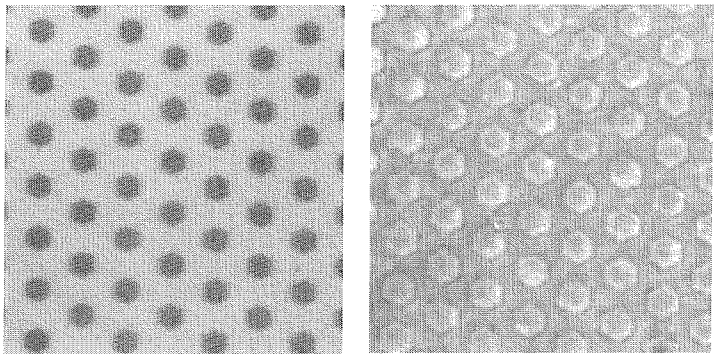

(a) (b)

Figure 1

Fig. 1. Optical microscopy images of the photolithography mask used in the fabrication process (a), and of the actual domain structure (b).

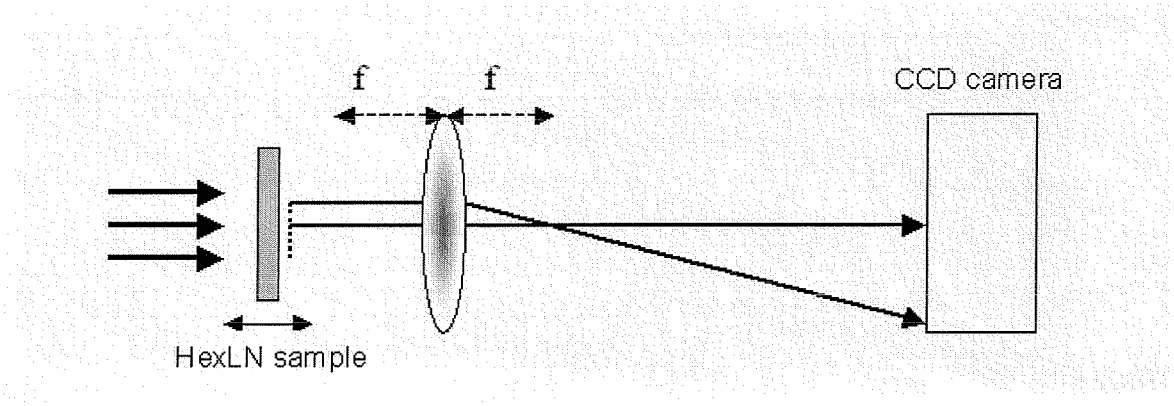

Figure 2

Fig. 2. Scheme of the used optical set-up.

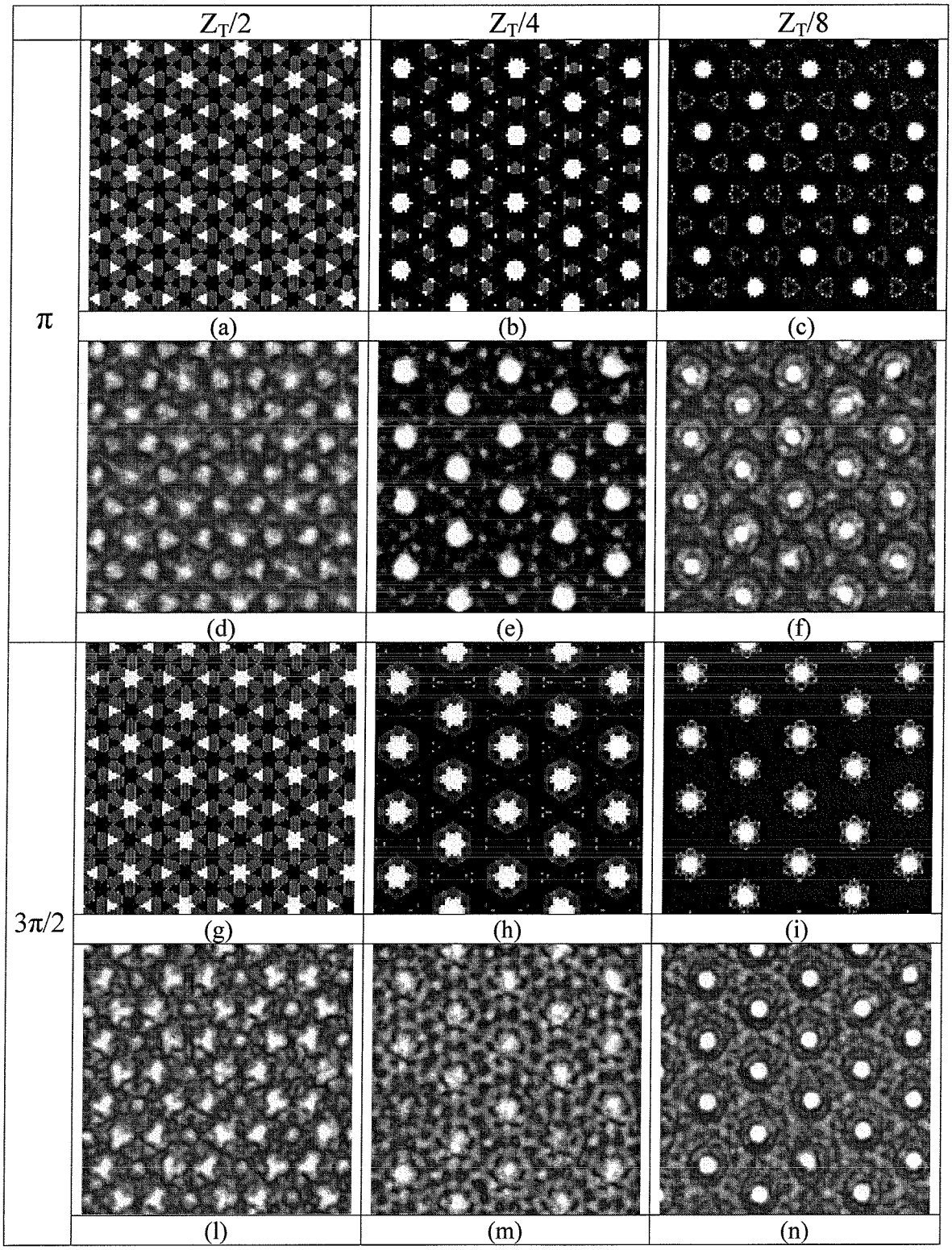

Figure 3

Fig.3. Experimental patterns obtained for a phase step $2\Delta\phi = \pi$ at $z = z_t / 2$ (a), $z = z_t / 4$ (b) and $z = z_t / 8$ (c) and the respective numerical simulations (d,e,f). Patterns obtained for a phase step $2\Delta\phi = 3\pi/2$ at $z = z_t / 2$ (g), $z = z_t / 4$ (h) and $z = z_t / 8$ (i) and the respective numerical simulations (l,m,n).

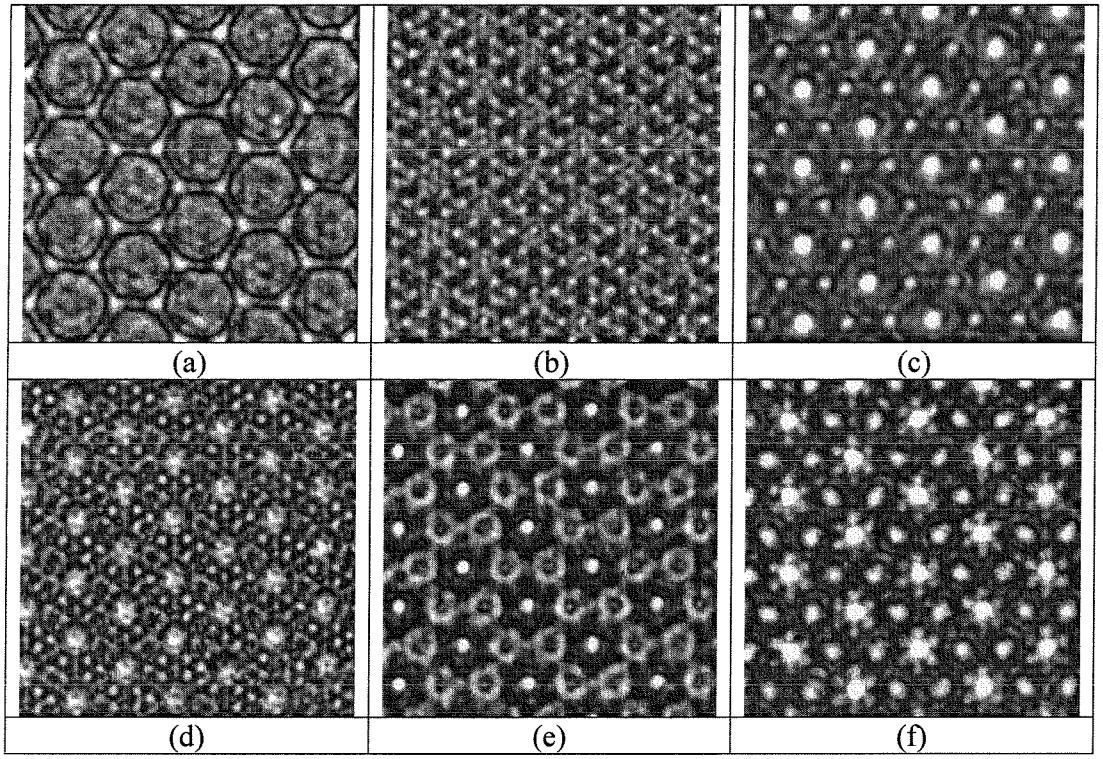

Figure 4

Fig. 4. A selection of interesting patterns obtained at different voltage and recording distances (see text)